BULLETIN OF THE POLISH ACADEMY OF SCIENCES
TECHNICAL SCIENCES, Vol. 63, No. 3, 2015
DOI: 10.1515/bpasts-2015-0079

An efficient algorithm for determining positions of astronomical objects in the Deep Sky Object pictures

R. SUSZYNSKI*, K. WAWRYN, and M. DZIEBOWSKI

Faculty of Electronics and Information Science, Koszalin University of Technology, 2. Sniadeckich St., 75-453 Koszalin, Poland

Abstract. The article presents an algorithm for digital image processing of astronomical objects in order to effectively determine the position of these objects. The proposed method has been optimized due to its effectiveness of removing noise and distortion caused by atmospheric turbulence and imperfections in long exposure photography of astronomical objects. This solution is ready for implementation in a system for automatic identification of stars in the recorded images. Such a system is designed for GoTo circuits at telescope's drives, which can automatically point a telescope to astronomical objects. The method was verified by simulation in MATLAB program on real images of astronomical objects.

Key words: effect of atmospheric turbulence, filtering of Deep Sky Object images, Gaussian noise.

1. Introduction

Astronomical images obtained with a telescope are subject to numerous distortions. These are brought on mainly by: atmospheric turbulence, noise, inherent noise of recording systems and imperfections of the optical system and drives. Obtaining the real picture is the task of adaptive optics (AO). It deals with filtering the interference from the received image, with determining the positions of deep sky objects (stars) and with generating a signal which corrects the optical system or the movement of the telescope tracking their location [1–4]. Determining the positions of stars, called the centroid detection, requires the determination of a reference point, i.e. a fixed element (a star) with respect to the photograph, which will set the position of the entire image, and thus the position of the other stars [5–7]. Detecting the position of the stars requires a calculation of their centers of gravity after removal of the distortion of the image. For this purpose, different calculation techniques are used. The simplest consists in determining the centers of gravity of stars [8] and its derivatives such as weighted centers of gravity, iteratively weighted centers of gravity or iterative weighted centroid [9–11]. Gaussian pattern matching is also used [12]. These methods are also preceded by calculations predicting the atmospheric turbulence (temperature oscillations and the influence of wind) by the Zernike polynomials [13], or Principal Component Analysis with Kalman filtering [14]. These are very time-consuming calculations, especially when the order of approximating polynomials is large. For predicting the turbulence, Bayesian estimation theory is also used [15].

The method of determining the position of stars proposed in this paper uses the method of filtration allowing to sufficiently compensate for the distortion caused by the previously mentioned factors, while providing results of the calculations in time to correct the motion of the telescope. The method is presented in the paper according to the following outline. Section 2 discusses the impact of atmospheric turbulence, inherent noise of the system, the imperfections of the optical and mechanical systems on the quality of the images received by the telescope, and presents simulations of the impact of atmospheric turbulence that was made on the recorded images. Noise filtering algorithm on the recorded images, together with determining the positions of astronomical objects is described in Sec. 3. In Sec. 4, the results of the algorithm are illustrated with photographs before and after the reconstruction and verified by comparison with the results obtained by standard methods [6, 7]. Section 5 contains conclusions.

2. Simulation of the impact of atmospheric turbulence on the quality of recorded images of astronomical objects

2.1. Image distortion in long exposure photography from the Earth surface. Obtained astronomical images require long time exposures, due to the small amount of light reaching the observer (CCD – Charge Coupled Device). This requires maintaining a still image that gets transferred to the CCD, for a period of a few to several dozens of minutes. It is a challenging task due to the apparent motion of the celestial sphere, associated with the rotation of the Earth. In order to maintain a steady image, appropriate assembly of optical systems (telescopes) is used, which follow the celestial sphere, according to the geographical position of the observations and the position of the observed object in the sky. Regardless of the correct installation of the telescope, astronomical images are distorted by atmospheric turbulence, inherent noise of the registering devices and inaccurate shooting.

Atmospheric turbulence is the main source of distortion. These distortions are caused by optical lenses emerging in the atmosphere, differences in temperature and density of

*e-mail: roberts@tu.koszalin.pl

the air at different heights, movements of atmosphere masses and dust and air pollution gases. Such distortions may also include distortions caused by light sources emerging in the immediate vicinity, i.e. municipal lighting, streets, commercials, flashes of light and reflections.

Inherent noise of registering devices has a statistical character described by the Poisson distribution. The signal-to-noise ratio is improved when more photons reach the CCD. The darker areas of the image are more noisy than lighter areas. In order to increase the amount of light reaching the image sensor, long exposure times are used.

Shooting inaccuracies are caused by mechanical vibrations of the telescope mounting drive, vibrations of the environment that get transferred to the drive and the optical system, as well as external factors influencing the drive-telescope-CCD camera system, such as wind, fast temperature fluctuations, changes in temperature, precipitation. A partial solution to these problems is building observation stations [16] equipped with more accurate telescopes mounts and isolating telescopes from the influence of the environment.

It is an extremely difficult task to reduce the impact of atmospheric phenomena on the quality of the photos. A compensation method for the distortions stemming from atmospheric turbulence is described further in the paper.

2.2. Simulation of the Earth's atmosphere on the recorded image of the stars. Ideally, the stars should be recorded on the image in the form of individual pixels with values corresponding to their relative brightness. Due to, among others, atmospheric turbulence, such ideal conditions do not exist, and the stars are recorded in the form of fuzzy points. In the description of such a blur, corresponding function describing the propagation of light is applied (PSF – *Point Spread Function*). In the vast majority of cases, Gaussian function is used, expressed with the relation [17, 18]:

$$\mu(x,y) = \frac{1}{2\pi\delta}\exp\left[-\frac{(x-X)^2+(y-Y)^2}{2\delta^2}\right] \qquad (1)$$

in which x and y are coordinates of pixel, δ is the standard deviation, and X and Y determine the center point for which there is the highest value of star brightness.

Such a description does not include a case when the main beam of light coming from the stars falls on a different point than the center pixel of the CCD. Because of this, the method was improved, and it shows as follows:

- In a graphic file, a pixel map with zero values, individual pixels are placed, with a value corresponding to the brightness and position of simulated stars,
- for each pixel representing the star, PSF Gaussian function is created, which describes the distribution of the light, wherein the standard deviation has a value dependent on the value of the pixel (i.e. the brightness of the star), then the values of this function are given to the pixels surrounding the pixel representing a star,
- then the $n \times n$ resolution of the pixel map is reduced, by imposing a grid consisting of frames with the dimension of $n \times n$ pixels; in each such frame, the pixel values are added, and the created sum, after normalization, constitutes the value of a newly created pixel,
- the new grid of pixels are multiplied by the value of the pixel corresponding to the parameters of the star, creating a simulation of a fuzzy image that arises in real conditions.

Figure 1 shows the actual captured image and the result of a simulation for stars of known location and relative brightness. In Fig. 1b, darker stars are omitted, as irrelevant to the subsequent stages of research. The resulting simulated images of stars correspond to their real prototypes in the actual image, in terms of brightness, surface and shape. Test image obtained in this way, as well as real images were used in the rest of the work to verify the algorithm determining the position of the stars.

a)

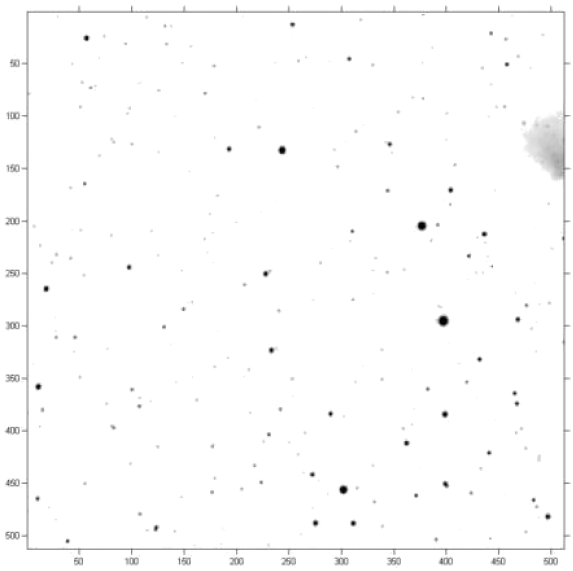

b)

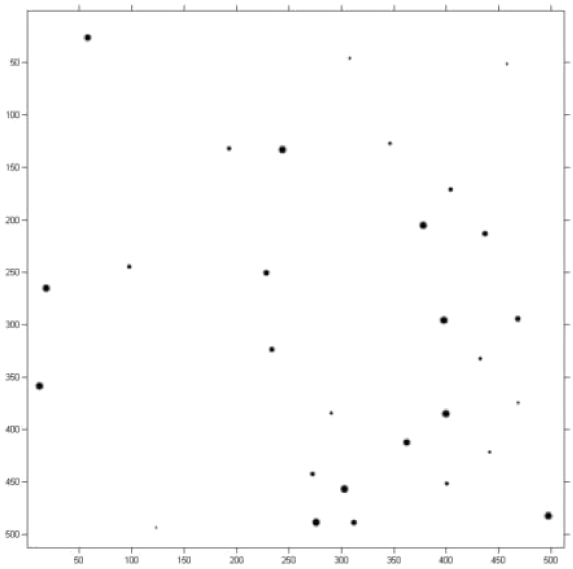

Fig. 1. The stars of the Milky Way, 512×512 pixels images: a) the real recorded image, b) calculated image based on the positions of stars and their relative brightness

3. Optimization of determining the position of stars

3.1. Filtration correcting the recorded image. In the first step in the digital processing a high-pass Laplacian filter [19] is applied. To process the reference picture an efficient image processing algorithm was used as described in [20]. The method uses two-dimensional (2D) filtering [21]. The following 2D transfer function matrix

$$\boldsymbol{H}(z_h, z_v) = \begin{bmatrix} 1 & z_h^{-1} & z_h^{-2} \end{bmatrix} \begin{bmatrix} -1 & -1 & -1 \\ -1 & 8 & -1 \\ -1 & -1 & -1 \end{bmatrix} \begin{bmatrix} 1 \\ z_v^{-1} \\ z_v^{-2} \end{bmatrix} \quad (2)$$

been used for preliminary filtering. The 2D transfer function has been decomposed into two cascaded one-dimensional (1D) transfer functions

$$\boldsymbol{H}(z_h, z_v) = \boldsymbol{H_h}(z_h)\boldsymbol{H_v}(z_v), \quad (3)$$

where $\boldsymbol{H_h}(z_h)$ and $\boldsymbol{H_v}(z_v)$ are horizontal and vertical vectors, respectively.

Next, 1D lossless matrices have been designed for both $\boldsymbol{H_h}(z_h)$ and $\boldsymbol{H_v}(z_v)$ and cascaded to determine Rosser's matrix

$$\boldsymbol{R} = \begin{bmatrix} \boldsymbol{A} & \boldsymbol{B} \\ \boldsymbol{C} & \boldsymbol{D} \end{bmatrix}, \quad (4)$$

where $\boldsymbol{A}$, $\boldsymbol{B}$, $\boldsymbol{C}$ and $\boldsymbol{D}$ denote matrices described in the Roesser state space model of 2D linear system [22] defined by the equations

$$\begin{cases} \begin{bmatrix} x^h(i+1,j) \\ x^v(i,j+1) \end{bmatrix} = \boldsymbol{A} \begin{bmatrix} x^h(i,j) \\ x^v(i,j) \end{bmatrix} + \boldsymbol{B}u(i,j) \\ y(i,j) = \boldsymbol{C} \begin{bmatrix} x^h(i,j) \\ x^v(i,j) \end{bmatrix} + \boldsymbol{D}u(i,j) \end{cases} \quad (5)$$

where i and j are integer-valued vertical and horizontal coordinates, respectively, $x^h(ij) \in R^h$ and $x^v(i,j) \in R^v$ are the horizontal and the vertical state vectors, respectively, $u(ij) \in R^m$ and $y(i,j) \in R^l$ are the input and the output vector, respectively, $\boldsymbol{A}$, $\boldsymbol{B}$, $\boldsymbol{C}$, $\boldsymbol{D}$ are real constant matrices of $r \times r$, $r \times l$, $k \times r$ and $k \times l$ dimensions, respectively.

Finally, the Roesser matrix has been rearranged to the following form

$$\boldsymbol{R} = \prod_{i=1}^{I} R_{s_i,t_i}(\phi_i)\, E \prod_{j=1}^{J} R_{u_j,w_j}(\varphi_j), \quad (6)$$

where

$$E = \begin{bmatrix} \pm 1 & 0 & \ldots & 0 \\ 0 & \pm 1 & \ldots & 0 \\ \ldots & \ldots & \ldots & \ldots \\ 0 & 0 & \ldots & \pm 1 \end{bmatrix},$$

$$R_{s,t}(\phi) = \begin{array}{c} \\ s \\ \\ \\ t \\ \\ \end{array} \begin{array}{c} \begin{array}{ccccccc} s & & & & t & & \end{array} \\ \begin{pmatrix} 1 & & & & & & \\ & \ddots & & & & 0 & \\ & & \cos\phi & & -\sin\phi & & \\ & & & 1 & & & \\ & & & & \ddots & & \\ & & \sin\phi & & \cos\phi & & \\ & 0 & & & & 1 & \\ & & & & & & \ddots \end{pmatrix} \end{array}.$$

The matrix $R_{s,t}(\phi)$ is known as Given rotation [23]. It can be implemented as transformation of two coordinates taken from s and t columns to perform rotation of 2D vector trough an angle ϕ. The matrix $R_{s,t}(\phi)$ is implemented by $I + J$ rotations.

This operation is not numerically intensive and not time consuming, given the small size of the mask used, but it improves the processed image. Filtering allows to highlight the central part of positioned objects, thereby increasing the confidence and efficiency of computing the centroid calculation in the following steps. Noise and interference are suppressed, which makes them easier to be removed. The subsequent stages of processing real star image photographed by the SBIG 2000XM camera and telescope SkyWatcher 80D are shown in Fig. 2. Image of the average brightness of the star was obtained by separating the frame size of 32×32 pixels with 5 minute exposure of the Milky Way in the Cygnus constellation. Figure 2a shows the image of a star before filtration. A blurring of light can be seen, surrounding its brightest central pixels with an area of 10×11 pixels. Such a large area of the registered object does not allow for an unambiguous determination of its position, without further signal processing. The next Fig. 2b shows the effect of filtration. A reduction and alignment of background levels can be seen, as well as reduction of blurring of the stars, while highlighting its brightest pixels.

3.2. Extracting useful signals from background noise and interference. In the second stage of the digital image processing of astronomical objects, the noise associated with the background should be removed. The easiest way to achieve this is to use the method of threshold segmentation, the threshold factor chosen according to the type of photographed subjects and image quality. Good results are achieved for the threshold in the range of 0.30–0.50 of the maximum recorded value.

This method has a major drawback. During the threshold segmentation information about weaker signals registered is irretrievably lost, that is about darker astronomical objects, captured in the images at the level of background noise. Reducing the threshold value allows to extract a larger number of objects (including darker ones), but introduces the danger of interpreting the interference signal (e.g. coming from hot pixels) as new objects. Since the aim of the image processing

algorithm presented here is an accurate positioning of only the brightest objects registered, this drawback in this case is not significant.

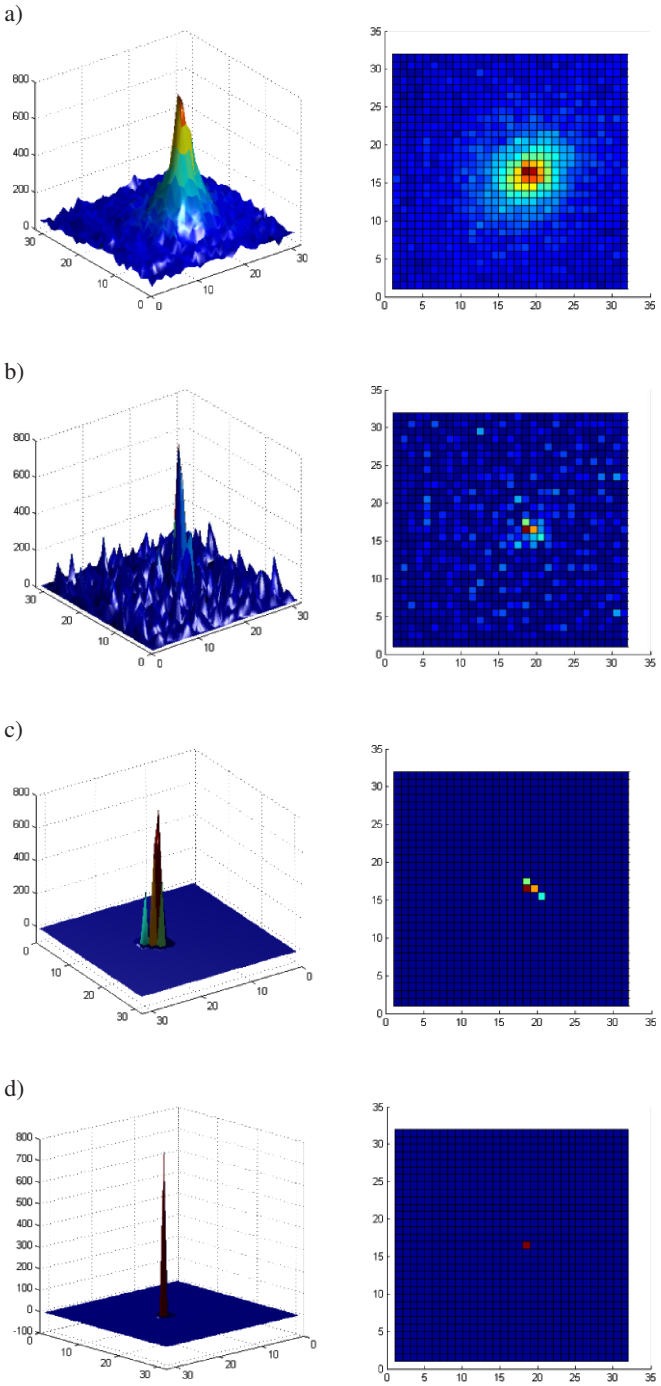

Fig. 2. The steps of determining the position of the stars, 32×32 pixels images: a) the real recorded image, b) image after filtering using the Laplacian, c) segmentation threshold, d) the designated centroid

3.3. Determining of the position of objects – centroid calculation. The final, third stage of calculations for the selected objects, is to determine their coordinates in the captured image. The process is performed by designating the weighted center of gravity, taking into consideration the brightness of each pixel in the object. The horizontal coordinate x_0 and the vertical coordinate y_0 of the object center can be calculated according to the formulas:

$$x_0 = \frac{\sum_{i=1,j=1}^{m,n} B_{ij} x_{ij}}{\sum_{i=1,j=1}^{m,n} B_{ij}} \tag{7}$$

and

$$y_0 = \frac{\sum_{i=1,j=1}^{m,n} B_{ij} y_{ij}}{\sum_{i=1,j=1}^{m,n} B_{ij}}, \tag{8}$$

where i, j are horizontal and vertical indexes of pixel of the selected object, B_{ij} is the brightness of the pixel i, j, x_{ij} is the horizontal coordinates of the pixel i, j, y_{ij} is the vertical coordinates of the pixel i, j.

Figure 2c reveals the effect of the segmentation with the threshold of 0.3. A small group of bright pixels is left for further analysis. The method of testing the background of non-zero pixels was as optimal in the proposed algorithm. It involves strengthening the brightest pixel in the group and dimming all the others. In Fig. 2d, the final result of the star's centroid calculation is shown. This is a single non-zero pixel determining the position of the star with an accuracy equal to the resolution used in the recorder.

4. Verification of the algorithm for the test image and real images of stars

The presented algorithm has been implemented numerically in MATLAB. As input images, real long exposure images of astronomical objects were used. They were registered by a SkyWatcher telescope with a SBIG 2000XM camera, on an equatorial mount SkyWatcher EQ6 PRO SynScan. For comparison, the same methods were applied to the test images, obtained by simulation of atmospheric effects, as described in Sec. 2. Figure 3a shows a test fragment (256x256 pixels) of the original image of objects in the Deneb star's environment, in the Cygnus constellation, prior to digital processing. The same stars after filtering, segmentation and centroid calculation are shown in Fig. 3b.

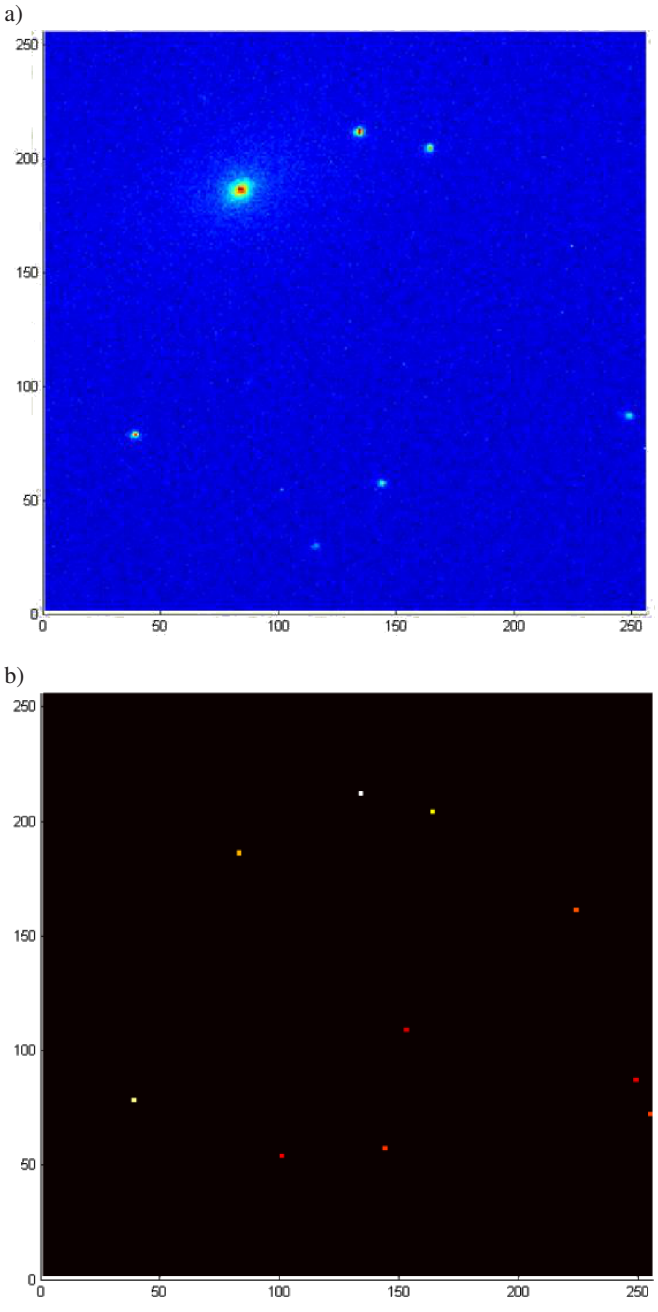

Fig. 3. Group of stars in the Cygnus constellation, 256×256 pixels images: a) the real recorded image, b) the final result of the stars' centroids calculation

Table 1 presents a summary illustrating the computational complexity of the proposed method with respect to the standard methods [6, 7, 24] described in the literature. For all the tested methods, calculations were performed for the real image in Figure 3a, and a generated test pattern. When comparing the obtained results, it can be noted that the current algorithm simplifies and accelerates the calculation, while maintaining satisfactory results and the accuracy of determining the position of the photographed objects. Approximate computation time and the number of mathematical operations necessary to implement each method were both obtained by developing an appropriate algorithms in Matlab and performing calculations using a workstation with two Xeon X5460@3.16GHz processors.

Table 1
Summary of computational complexity of the proposed method and the classical methods

Method/Computational complexity	The proposed algorithm	Correlation coefficient method	FFT method
Number of summations	2 297 284	78 848 000	2 241 300
Number of multiplications	129 032	26 215 200	14 293 665
Approximate calculation time	0.3171 s	1.8085 s	0.7932 s

5. Conclusions

The paper presents an efficient algorithm for determining the positions of astronomical objects in the sequence of long exposure photographs of Deep Sky Objects. The algorithm has been optimized for the use in systems of tracking stars working in real-time. The development of efficient numerical methods for filtering, segmentation and identification allows for a precise calculation of the position of the tested objects and for applying the method in real-time systems [25, 26] using DSP, FPAA or FPGA.

REFERENCES

[1] G.D. Roth, *Handbook of Practical Astronomy*, Springer-Verlag, Berlin, 2009.

[2] H.G. Ziegler, *Telescope Mountings, Drives, and Electrical Equipment*, *Compendium of Practical Astronomy*, vol. 1, chap. 5, Springer, Berlin, 1994.

[3] R. Suszynski, "A stand-alone station and DSP method for deep sky objects astrophotography", *Int. J. Electronics and Telecommunications* 60 (2), 157–164 (2014).

[4] R. Suszynski, "Digital processing of CCD images for autoguiding astrophotography system", *Proc. 15th Int. Conf. on Mixed Design of Integrated Circuits and Systems (MIXDES)* 1, 559–562 (2008).

[5] R. Suszynski, K. Wawryn, and R. Wirski, "2D signal processing for identification and tracking moving object", *Przegląd Elektrotechniczny* 87 (10), 126–129 (2011).

[6] R. Suszynski, "Convolution method for CCD images processing for DSO astrophotography", *Proc. IEEE 52nd Int. Midwest Symp. Circuits and Systems (MWSCAS)* 1 (4), 762–765 (2009).

[7] R. Suszynski and K. Wawryn, "An improvement of stars' centroid determination using PSF-fitting method", *Proc. IEEE Int. Conf. Signals and Electronics Systems ICSES* 1, 4 (2014).

[8] P.C. McGuire, D.G. Sandler, M.L. Hart, and T.A. Rhoadarmer, "Adaptive optics: neural networks wavefront sensing, reconstruction, and prediction", *Proc. 194th W.E. Heracus Seminar* 1, CD-ROM (1998).

[9] S. Thomas, T. Fusco, A. Tokovinin, M. Nicolle, V. Michau, and G. Rousset, "Comparison of centroid computation algorithms in a Shack-Hartmann sensor", *Monthly Notices of the Royal Astronomical Society* 371, 323–336 (2006).

[10] K.L. Baker and M.M. Moalem, "Iteratively weighted centroid of Shack-Hartmann wave-front sensors", *Opt. Express* 15, 5147–5159 (2007).

[11] L.A. Poyneer, D.W. Palmer, K.N. LaFortune, and B. Bauman, "Experimental results for correlation-based wave-front sensing", *SPIE Advanced Wavefront Control* 5894, 58940N (2005).

[12] A. Vyas, M.B. Roopashree, and B.R. Prasad, "Cetroid detection by Gaussian pattern matching in adaptive optics", *Int. J. Computer Applications* 1, 30–36 (2010).

[13] R.J. Noll, "Zernike polynomials and atmosphere turbulences", *JOSA* 66, 207–211 (1976).

[14] A. Berghi, A. Canedese, and A. Masiero, "Atmospheric turbulence prediction: a pca approach", *Proc. IEEE 46th Conf. Decision and Control* 1, 572–577 (2007).

[15] B.D. Jeffs and J.C. Christou, "Blind bayesian restoration of adaptive optics telescope images using generalized gaussian markov random field models", *Proc. Conf. on Adaptive Optics and Telescope Systems SPIE* 3353, CD-ROM (1998).

[16] R. Suszynski, "Stand-alone station for deep space objects astrophotography", *Proc. IEEE 52nd Int. Midwest Symposium on Circuits and Systems (MWSCAS)* 1 (4), 333–336 (2009).

[17] W. Zhang, Z. Jiang, H. Zhang, and J. Luo, "Optical image simulation system for space surveillance", *Proc. IEEE 26th Int. Parallel and Distributed Processing Symp.* 1, CD-ROM (2012).

[18] C. Li, Y. Zhang, C. Zheng, and X. Hu, "Implementing high-performance intensity model with blur effect on gpus for large-scale star image simulation", *Proc. Int. Conf. on Image and Graphics* 1, CD-ROM (2013).

[19] R. Szeliski, *Computer Vision, Algorithms and Applications*, Springer-Verlag, London, 2011.

[20] R. Suszynski, K. Wawryn, and R. Wirski, "2D image processing for auto-guiding system", *Proc. IEEE 54th Int. Midwest Symp. on Circuits and Systems MWSCAS* 1, CD-ROM (2011).

[21] K. Wawryn, R. Wirski, and B. Strzeszewski, "Implementation of finite impulse response systems using rotation structures", *Proc. Int. Symp. Information Theory and Its Applications ISITA2010* 1, CD-ROM (2010).

[22] R.P. Roesser, "A discrete state-space model for linear image processing", *IEEE Trans. Automat. Contr.* 20, 1–10 (1975).

[23] D.E. Dudgeon and R.M. Mersereau, *Multidimensional Signal Processing*, Prentice-Hall, Englewood Cliffs, 1984.

[24] Ch.-S. Li and S-Z. Jin, "The implement of high speed correlation tracking algorithm based on FPGA in space solar telescope", *Proc. 8th Int. Conf. on Signal Processing* 1, CD-ROM (2006).

[25] K. Wawryn and R. Suszynski, "Low power 9-bit pipelined A/D and 8-bit self-calibrated D/A converters for a DSP system", *Bull. Pol. Ac.: Tech.* 61 (4), 979–688 (2013).

[26] R. Suszynski and K. Wawryn, "Rapid prototyping of algorithmic A/D converters based on FPAA devices", *Bull. Pol. Ac.: Tech.* 61 (3), 691–696 (2013).